

Extragalactic symbiotic systems*

IV. The supersoft X-ray source SMC 3

Stefan Jordan¹, Werner Schmutz², Burkhard Wolff¹, Klaus Werner^{1,3}, Urs Mürset²

¹ Institut für Astronomie und Astrophysik, Universität Kiel, D-24098 Kiel, Germany

E-mail: jordan/wolff/werner@astrophysik.uni-kiel.d400.de

² Institut für Astronomie, ETH Zentrum, CH-8092 Zürich, Switzerland; E-mail: schmutz/muerset@astro.phys.ethz.ch

³ Lehrstuhl Astrophysik, Universität Potsdam, Am Neuen Palais 10, D-14469 Potsdam, Germany

Received, accepted

Abstract. We present a consistent model for the UV and supersoft X-ray emission from the symbiotic nova SMC3 (= RX J0048.4–7332). Following the present picture of symbiotic stars, the model consists of radiation from a hot star and an emission nebula excited by that star. The observations were compared to theoretical models in which the hot star's emission is calculated with the help of hydrostatic and Wolf-Rayet-type non-LTE model atmospheres. Our analysis clearly shows evidence for mass loss rates of several $10^{-6} M_{\odot}/\text{yr}$. The minimum effective temperature compatible with both the observed UV and X-ray flux is about 260 000 K, which is higher than in any other star analyzed with sophisticated NLTE model atmospheres. Since the hydrostatic surface is hidden by the stellar wind no upper limit for the temperature can be determined. However, we were able to determine the total luminosity of a symbiotic nova with reasonable accuracy ($L_{\text{SMC3}} = 10^{4.05 \pm 0.05} L_{\odot}$). This value is well below the Eddington limit ($\approx 50 000 L_{\odot}$). In order to reproduce the observed energy distribution a carbon-to-helium ratio $> 2 \cdot 10^{-4}$ — leading to an absorption edge at 0.39 keV — is necessary.

Key words: Binaries: symbiotic – Stars: fundamental parameters – Stars: Individual: SMC3 – Stars: Individual: RX J0048.4–7332 – Stars: mass-loss – X-rays: stars

1. Introduction

ROSAT observations established the class of ‘supersoft X-ray sources’ (‘SSS’; e.g. Hasinger 1994) with almost no flux

Send offprint requests to: S. Jordan

* Based on data collected with the ROSAT and the IUE satellites

at $h\nu \geq 0.5 \text{ keV}$; normally, close-by low-luminosity objects like single white dwarfs or cool coronal stars are excluded from this definition. The nature of many SSS is still a matter of controversial discussion. RX J0048.4–7332 is one of ten SSS confirmed as members of the Magellanic Clouds (Kahabka & Pietsch 1993; Pietsch & Kahabka 1993). In this paper we investigate the hypothesis that the X-ray flux of this object is due to photospheric emission of a very hot white dwarf. Given a sufficiently high temperature the photospheric emission of white dwarfs is measurable in the ROSAT window (e.g. Jordan et al. 1994b, Wolff et al. 1996). A hot white dwarf is hardly the correct explanation for all supersoft X-ray sources. However, at least for some sources, the presence of a very hot star is also in agreement with other evidence: For instance, in symbiotic systems there are high excitation nebular emission lines combined with a hot continuum in the UV. The supersoft appearance is also expected from the theoretical side; in particular, for symbiotic novae Sion & Starrfield (1994) predict phases in which a very hot white dwarf can be detected.

Indeed, the supersoft source RX J0048.4–7332 coincides with the symbiotic nova SMC3 that has been in outburst since 1981 (Morgan 1992). Thus, for this system it appears natural to propose that a hot white dwarf is the source of the X-ray flux. Symbiotic stars are interacting binaries consisting of a red giant and a very hot white dwarf (typically $T_{\text{eff}} \sim 100 000 \text{ K}$), whose radiation ionizes the emission nebula. In the optical spectral range we observe a composite spectrum from the cool star and the nebula. The UV spectrum is dominated by the nebular emission with only a small contribution from the hot star that becomes dominant at the shortest wavelengths. The spectral range best suited for a direct observation of the hot component of a symbiotic system is the soft X-ray and EUV part of the electromagnetic spectrum, where these

stars emit the bulk of their energy (e.g. RR Tel, see Jordan et al. 1994a, hereafter JMW).

Vogel & Morgan (1994; Paper I) obtained an IUE spectrum of SMC3 which looks typical for a symbiotic star of moderate excitation. On the other hand, the optical spectrum (Morgan 1992; Mürset et al. 1995 = Paper III) reveals nebular ionization that is unusually high for symbiotics, up to Fe^{+9} . Even more peculiar, however, are the X-ray observations presented by Kahabka et al. (1994): Despite of the large distance, the ROSAT count rate of SMC3 is about the same as of RR Tel, hitherto the X-ray brightest of all known galactic symbiotic novae (Jordan et al. 1994a; hereafter JMW). Thus, the ratio of the optical to the X-ray flux of SMC3 is a challenge for models of symbiotic stars. On the other hand, the known distance of this extragalactic system provides a unique opportunity to investigate the energetics of interactions and outbursts in symbiotic systems.

Kahabka et al. (1994) have presented black body fits to the ROSAT data, which resulted in an extremely unrealistic luminosity of up to 10^{13} L_\odot . However, we will show that a reasonable value is obtained if the data are compared to appropriate model atmospheres, and if we consistently take into account the constraints from both the X-ray and UV regions of the electromagnetic spectrum.

In Sect. 2 we list the data used in our analysis, in Sections 3 and 4 we describe the methods, the results are discussed in Sect. 5, and Sect. 6 presents some concluding remarks.

2. Data

2.1. ROSAT

Pointed ROSAT PSPC observations were retrieved from the ROSAT archive and reduced using the EXSAS software (Zimmermann et al. 1994). Kahabka et al. (1994) describe the data, obtained during a 20 ks exposure in April 1992, in detail. We binned the counts into the various energy channels until a signal-to-noise ratio of five was achieved. After correcting for dead time and vignetting the resulting total count rate amounts to 0.204 ± 0.004 counts/sec. The observed PSPC pulse height distribution (PHD) is displayed in Figs. 2 – 6.

A follow-up observation in December 1992 is not included in the archive by the time of writing, and could therefore not be used for this work.

2.2. IUE

The UV spectrum of SMC3 is described in Paper I. It was observed with the short wavelength ($1200 \text{ \AA} \lesssim \lambda \lesssim 1900 \text{ \AA}$) camera of the International Ultraviolet Explorer satellite (IUE) at low resolution using the large ($20'' \times 10''$) aperture in April 1993. Given the stability of SMC3 in its present outburst stage (Morgan 1992) we assume that

there was no variability so that the ROSAT and the UV observation can be combined.

2.3. Optical spectra

Optical low resolution spectra of SMC3 have been published by Morgan (1992) and in Paper III. The spectrum is typical for a high excitation s-type symbiotic. It displays H I Balmer, He I, and He II emission lines, as well as the Raman scattered O VI $\lambda\lambda 6825, 7082$ features (cf. Schmid 1989). In addition to the typical features, [Fe X] $\lambda 6374$ is also present which is very rarely observed in symbiotic spectra. Davidsen et al. (1977) report [Fe X] emission from GX1+4, which is a symbiotic system that contains a neutron star, and Webster & Allen (1975) observed [Fe X] for He2-171. The spectrum of AS 295B contains [Fe X], [Fe XI], and [Fe XIV] (Herbig & Hoffleit 1975).

From the $\text{H}\beta$ luminosity and the line ratios given by Morgan (1992) we derive the optical line fluxes of $\text{H}\beta$ and He II $\lambda 4686$ listed in Table 1.

Table 1. Continuum and integrated emission line fluxes from SMC3 used in the analysis. The optical line fluxes are from Morgan (1992).

$f(\text{continuum } \lambda = 1300 \text{ \AA})$	$2.9 \cdot 10^{-15} \text{ erg cm}^{-2} \text{ s}^{-1} \text{ \AA}^{-1}$
$f(\text{He II } \lambda 1640)$	$2.3 \cdot 10^{-13} \text{ erg cm}^{-2} \text{ s}^{-1}$
$f(\text{He II } \lambda 4686)$	$3.3 \cdot 10^{-14} \text{ erg cm}^{-2} \text{ s}^{-1}$
$f(\text{H}\beta \lambda 4861)$	$4.5 \cdot 10^{-14} \text{ erg cm}^{-2} \text{ s}^{-1}$
$f(\text{[Fe X] } \lambda 6374)$	$2.0 \cdot 10^{-14} \text{ erg cm}^{-2} \text{ s}^{-1}$

2.4. Distance and interstellar extinction

Our analysis requires reddening corrected continuum and emission line fluxes. The extinction can be derived by comparing the flux ratio of the He II recombination lines $\lambda 4686$ and $\lambda 1640$ to the theoretical value for case-B recombination (Hummer & Storey 1987). Although this ratio implies negligible extinction, we corrected for the foreground extinction of the SMC ($E_{\text{B-V}} = 0.05$; Bessell 1991) by using a galactic extinction curve, and subsequently applying the SMC extinction curve by Prévôt et al. (1984) for $E_{\text{B-V}} = 0.03$, which is the average internal extinction of the SMC (Bessell 1991). For the distance to the SMC we adopt $d = 61$ kpc determined by Barnes et al. (1993).

3. Atmospheres

The spectroscopic analysis is based on state-of-the-art non-LTE atmospheres as required by the high temperatures involved. They were calculated with two different

codes, one assuming plane-parallel geometry and hydrostatic layers, the other is appropriate for extended atmospheres with a steady state stellar wind. Table 2 gives an overview on the hot model atmospheres that have been calculated.

3.1. Hydrostatic models

As in the case of RR Tel (JMW) we first computed the theoretical model spectra for the hot stellar component with line blanketed non-LTE model atmospheres assuming plane-parallel geometry and hydrostatic and radiative equilibrium. Besides hydrogen and helium the models contain C, N, and O. The number of non-LTE levels assigned to each species are 5, 12, 38, 48, 48, respectively, and a total of 333 lines were explicitly included. The characteristics of these models were described in detail by Werner & Heber (1991).

3.2. Models with a stellar wind

Plane-parallel models are justified if the thickness of the stellar atmosphere is small compared to the stellar radius. This is normally the case for hot white dwarfs. However, these assumptions may not be valid in the case of a symbiotic nova, since for several of the symbiotic novae, there is evidence for mass loss (e.g. Nussbaumer et al. 1995, Nussbaumer & Vogel 1995). Therefore, we also calculated models with mass loss as an additional free parameter using the co-moving frame code for hot stars with a strong stellar wind developed in Kiel (Hamann & Schmutz 1987; Wessolowski et al. 1988). The non-LTE calculations include 6 levels for the hydrogen model atom; 11 levels for helium with 5 levels for He I and 5 levels for He II; 12 levels for carbon with 5 levels for C IV and 6 levels for C V; 6 levels for nitrogen (5 levels for N V) and 9 levels for oxygen (5 levels for O VI). In total 44 levels and 54 line transitions are treated explicitly.

The free parameter of a model with an extended atmosphere due to mass loss are T_{eff} , R_* , \dot{M}/v_∞ , and β . The radius, R_* , is the inner boundary of the model. This inner boundary is either where the expansion velocity of the envelope is subsonic or, if the mass loss is so strong that this region is at very large optical depths, then the inner boundary is set where the Rosseland optical depth $\tau_R \approx 100$. The temperature T_{eff} yields in combination with R_* the luminosity. v_∞ and β specify the velocity law of the wind. We adopt a velocity law $v(r) = v_\infty(1 - R_*/r)^\beta$, assuming $\beta = 1$ and $v_\infty = 1000$ km/sec (cf. section 5.2). This type of law resembles that found empirically for O stars (Groenewegen & Lamers 1989) and agrees with the law calculated hydrodynamically for radiation driven winds of O stars (Pauldrach et al. 1986; Schaefer & Schmutz 1995).

4. Fit procedure

There are three observational constraints that have to be reproduced by a successful model: the X-ray flux, the UV continuum in the IUE wavelength range, and the nebular emission line He II $\lambda 1640$; in addition, there is a high ionization line, [Fe X] $\lambda 6374$. Since a forbidden transition is very sensitive to the unknown density of the nebula, the observation of the [Fe X] line implies only a lower limit for the hardness of the exciting radiation, but the observed line strength does not help to constrain a stellar parameter.

In order to reproduce the three observations we have adapted the following procedure. First, we have computed a large grid of model atmospheres with different parameters in T_{eff} , $\log g$, chemical composition, and mass loss rates (or \dot{M}/v_∞ , respectively).

The emergent flux does not depend on the radius of the models. This is obviously true for hydrostatic models where the radius is not among the model parameters. But, it is also correct for spherically extended models with mass loss, provided that the product $\dot{M}/v_\infty/R_*^{3/2}$ is kept constant (Schmutz et al. 1989). Thus, if we assume that the continuum at $\lambda = 1300$ Å is dominated by the flux of the hot star, we can compute the stellar radius for each model, knowing the flux predicted by the model atmosphere and the observed luminosity at 1300 Å; at this wavelength the hot stellar emission dominates the continuum in all symbiotic objects whose UV spectra have been investigated by Mürset et al. (1991).

With the absolute dimensions of the star determined by the observed 1300 Å flux for each model of the grid, we fed the emergent radiation to the photo-ionization code NEBEL (Nussbaumer & Schild 1981; Deuel 1986; Vogel 1990). For the calculation of the emission lines we assume that the nebula is radiation bounded in the He II region. We have no possibility to verify this assumption. However, Mürset et al. (1991) found the He II region to be radiation bounded for almost all symbiotic systems and only a few exceptions being nearly radiation bounded. The presence of a radiation bounded nebula is in no contradiction to the observed X-rays since our calculations show that an ionization bounded nebula is not necessarily optically thick below 100 Å; material from the neutral part of the nebula does, of course, contribute to the column density towards the X-ray source. Indeed, we find hydrogen column densities (up to $1.1 \cdot 10^{21}$ cm $^{-2}$) that are much larger than the value we would expect from the reddening of SMC3 (the formula by Groenewegen & Lamers 1989 yields about $N_{\text{H}} = 1.9 \cdot 10^{20}$ cm $^{-2}$ for $E_{\text{B-V}} = 0^m05$). We interpret the large hydrogen column densities as evidence for the symbiotic nebula being radiation bounded.

The strength of the He II $\lambda 1640$ line is a measure for the number of stellar photons emitted below $\lambda = 228$ Å, but weighted strongly for photons just shortwards of the threshold wavelength. Thus, basically, we use a sophisti-

cated Zanstra method. As it is the case for the original Zanstra method, our analysis depends only weakly on the adopted parameters of the nebula. A comparison of the calculated He II $\lambda 1640$ line flux with the observed one selects those models with the correct number of He⁺ ionizing photons.

For a black body energy distribution the He II $\lambda 1640$ analysis yields a unique temperature. If we use emergent radiation from hydrostatic atmospheres, the He II $\lambda 1640$ analysis selects different effective temperatures depending on the chemical composition of the atmosphere and – to a much lower degree – on the gravity. However, although there is a range of temperatures of plane-parallel models that fits the observed He II $\lambda 1640$ flux, the He II $\lambda 1640$ analysis still determines the stellar temperature reasonably well.

The results using atmospheres with a stellar wind differ fundamentally from those based on plane-parallel models. If we feed the model flux resulting from our calculations with extended model atmospheres with mass loss to the He II $\lambda 1640$ analysis, we find that the number of He⁺ ionizing photons is a sensitive function mainly of the mass loss, and not of the stellar temperature (see Sect. 5.3). The flux below 228 Å is suppressed by absorption in the wind depending on the mass loss rate. If the mass loss rate is sufficiently large helium recombines to He⁺ and in this case, the wind is optically thick to photons more energetic than the He⁺ edge (Schmutz et al. 1992). In Fig. 1 we show the EUV and soft X-ray energy distribution predicted by three models with about the same effective temperature of $T_{\text{eff}} = 300,000$ K but different mass loss rates (models x – z). Thus, for wind models the He II $\lambda 1640$ analysis does not provide information on the effective temperature except that there is a lower limit in order to produce He⁺ ionizing radiation. However, no upper limit to the effective temperature of the star can be specified: We can always increase the mass loss rate to reduce the number of He⁺ ionizing photons to the value implied by the observed He II $\lambda 1640$ flux, no matter what stellar temperature we choose.

The third step of our analysis is to compare the X-ray flux of the model atmosphere with the flux observed by ROSAT. For this comparison the theoretical spectrum has to be attenuated to account for the absorbing interstellar and circumstellar material. We calculate the absorption according to Morrison & McCammon (1983) and Crudace et al. (1974). The attenuated spectrum is then converted to a pulse height distribution (PHD) by convolution with the PSPC detector response matrix and the effective areas provided by the EXSAS package. The comparison of the theoretical PHD with the low energy part of the ROSAT observation, 0.1 to 0.2 keV, allows to determine the hydrogen column density. The comparison of the high energy part tests the emergent flux of our models at wavelengths where the flux is sensitive to the stellar

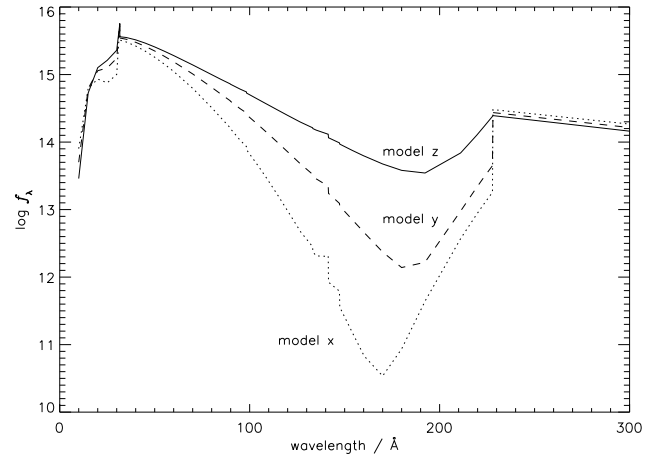


Fig. 1. Relative energy distributions of three models with approximately the same effective temperature of $T_{\text{eff}} = 300$ kK but with different mass loss rates (model x : $\dot{M}_x = 10^{-5.1} M_{\odot}/\text{yr}$, y : $\dot{M}_y = 10^{-5.2} M_{\odot}/\text{yr}$, and z : $\dot{M}_z = 10^{-5.3} M_{\odot}/\text{yr}$; see Table 2 for the other parameters). Note that a final velocity of $v_{\infty} = 1000$ km/sec is assumed (only \dot{M} / v_{∞} enters as a parameter into the model calculation)

temperature and to the presence of metals (e.g. the C⁺⁴ ionization edge at 0.39 keV).

5. Results

In Table 2 we list those parameter ranges for which we have calculated model atmospheres and for which the predicted flux distribution is able to reproduce the observed continuum flux at 1300 Å as well as the He II $\lambda 1640$ line flux. For these models the predicted X-ray luminosity was compared to the ROSAT observations. In Table 3 we summarize the results of these fits, and list the resulting T_{eff} and L_* , and for the models with stellar wind \dot{M} / v_{∞} . Also shown is the hydrogen column density required to fit the low energy X-ray part. In principle we could quantify the quality of the fits by listing the reduced χ^2 of the solution. However, one can clearly see that the deviations between the predictions and the observations are not solely due to statistical errors: Even in the case of the “relative good fits” systematic deviations remain which may have its origin in small incompleteness of the modelling. Finally, Table 2 comments on the quality of the resulting fit to the “high”-energy tail X-ray flux.

5.1. Black body emission

If we assume that the radiation of the hot component has a black body spectral distribution the He II $\lambda 1640$ analysis yields a unique solution, namely $T_{\text{BB}} = 100,000$ K and $R = 0.3 R_{\odot}$. However, the emergent X-ray flux of this

Table 2. Summary of model atmospheres parameters. In each series we computed atmospheres of several temperatures until a fit to the UV continuum and the He II emission could be achieved. The chemical abundances are given as number fractions.

Series	Model type	$\log \dot{M} / v_\infty$ [$M_\odot / (\text{yr km sec}^{-1})$]	$\log g$	β	H	He	C [10^{-5}]	N [10^{-5}]	O [10^{-5}]	Abundances similar to
<u>A</u>	hydrostatic	-	5 – 7	-	0.90	0.10	48.00	10.00	84	Sun
<u>B</u>	hydrostatic	-	6	-	0.90	0.10	4.80	1.00	8.4	Magellanic Clouds
<u>C</u>	hydrostatic	-	7.5	-	1.00	0.00	0.00	0.00	0.00	DA
<u>D</u>	hydrostatic	-	6 – 7.5	-	0.01	0.99	100.00	0.00	0.00	DO
<u>E</u>	hydrostatic	-	6 – 7	-	0.01	0.99	0.10	0.00	0.00	DO
<u>F</u>	hydrostatic	-	5.5 – 6	-	0.67	0.33	10.00	0.00	0.00	DO
<u>G</u>	hydrostatic	-	6	-	0.50	0.50	100.00	0.00	0.00	DO
<u>H</u>	hydrostatic	-	6 – 7	-	0.50	0.50	10.00	0.00	0.00	DO
<u>p</u>	WR-type	-8.53	-	1	0.50	0.50	40.00	0.76	7.50	-
<u>q</u>	WR-type	-8.50	-	1	0.50	0.50	40.00	0.76	7.50	-
<u>r</u>	WR-type	-8.12	-	1	0.50	0.50	100.00	0.76	100.00	-
<u>s</u>	WR-type	-7.97	-	1	0.50	0.50	200.00	0.76	100.00	-
<u>t</u>	WR-type	-8.30	-	1	0.50	0.50	20.00	0.76	7.50	-
<u>u</u>	WR-type	-8.30	-	1	0.50	0.50	40.00	0.76	7.50	-
<u>x</u>	WR-type	-8.10	-	1	0.50	0.50	40.00	0.76	7.50	-
<u>y</u>	WR-type	-8.20	-	1	0.50	0.50	40.00	0.76	7.50	-
<u>z</u>	WR-type	-8.30	-	1	0.50	0.50	40.00	0.76	7.50	-

Table 3. Solutions to the UV continuum and He II $\lambda 1640$ emission. The 5th column tells us whether a fit to the ROSAT observation could be achieved. The comment ‘too soft’ means that too much counts are predicted at low energies compared to the observation. Column 6 lists the implied interstellar hydrogen column density.

Model	Model type	T_{eff} [kK]	L_* [L_\odot]	Comment on implied ROSAT solution	N_{H} [10^{20} cm^{-2}]	Fig.
Black Body	Black Body	100	8 100	count rate is by far too low	< 0.1	-
<u>A</u>	hydrostatic	100	11 000	count rate is too low	0.0	-
<u>B</u>	hydrostatic	120	17 000	synthetic PHD is too soft	0.1	-
<u>C</u>	hydrostatic	65	5 800	synthetic PHD too low at 0.3–0.4 keV	0.4	-
<u>D</u>	hydrostatic	130	23 000	synthetic PHD too low at $E \gtrsim 0.25$ keV	4.0	2
<u>E</u>	hydrostatic	120	17 000	synthetic PHD too low at $E \gtrsim 0.20$ keV	1.7	2
<u>F</u>	hydrostatic	120	17 000	synthetic PHD too low at $E \gtrsim 0.20$ keV	2.0	
<u>G</u>	hydrostatic	120	16 000	synthetic PHD too low at $E \gtrsim 0.20$ keV	2.1	
<u>H</u>	hydrostatic	120	17 000	synthetic PHD too low at $E \gtrsim 0.20$ keV	2.6	
<u>p</u>	WR-type	220	9 200	PHD slightly too low at 0.20–0.45 keV	7.7	3
<u>q</u>	WR-type	265	10 200	PHD slightly too low at 0.30–0.45 keV	8.7	4
<u>r</u>	WR-type	309	11 200	relative good fit	8.8	3
<u>s</u>	WR-type	354	12 700	relative good fit	9.3	3
<u>t</u>	WR-type	300	16 800	PHD too high at $E > 0.45$ keV	8.8	6
<u>u</u>	WR-type	300	16 800	PHD slightly too low at 0.30–0.42 keV	8.8	6
<u>x</u>	WR-type	315	11 500	PHD too high at $E > 0.37$ keV	11.0	1, 5
<u>y</u>	WR-type	325	16 000	PHD too high at $E > 0.35$ keV	11.0	1, 5
<u>z</u>	WR-type	335	22 900	PHD too high at $E > 0.33$	11.0	1, 5

solution is much too low to reproduce the PSPC count rate, even for a vanishing interstellar hydrogen column density. Moreover, no [Fe x] emission is expected because the radiation field is not hard enough to produce Fe^{+9} .

Good fits to the PHD can be achieved if either the stellar radius is increased to about $1.5 \cdot 10^7 R_\odot$ or the temperature is increased to $T_{\text{BB}} \gtrsim 220,000 \text{ K}$ (with $R \approx 2 R_\odot$),

in agreement with the result seen in Fig. 1 of Kahabka et al. (1994). On obvious reasons, these parameters clearly lead to an UV flux several orders of magnitude too high compared to the observation. Also, the luminosity would exceed the Eddington limit by many orders of magnitude.

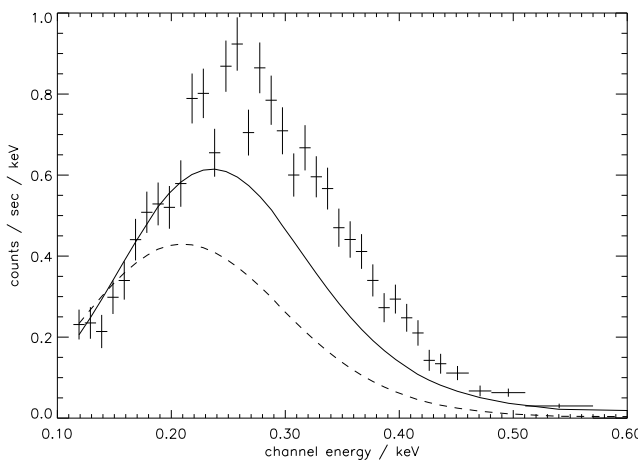


Fig. 2. The solid line is the best solution to the UV and X-ray observations with DO model atmospheres (model D in Tab. 2): $\text{He/H} = 100$, $\text{C/H} = 0.1$, $T_{\text{eff}} = 130,000 \text{ K}$, and $N_{\text{H}} = 4.0 \cdot 10^{20} \text{ cm}^{-2}$. Also shown is one example for another chemical composition (dashed line, model E): $\text{He/H} = 100$, $\text{C/H} = 10^{-4}$, $T_{\text{eff}} = 120,000 \text{ K}$, and $N_{\text{H}} = 1.7 \cdot 10^{20} \text{ cm}^{-2}$. The other compositions result in nearly the same synthetic PHDs

5.2. Hydrostatic models

Models with solar abundances (series A, see Tab. 3) lead to results similar to the black body case: the UV measurements would result in $T_{\text{eff}} \approx 100,000 \text{ K}$ whereas $T_{\text{eff}} \gtrsim 200,000 \text{ K}$ is needed to reproduce the X-ray observations. If we reduce the CNO abundances by a factor 10 (series B), the UV measurements are in agreement with the predictions at $T_{\text{eff}} \approx 120,000 \text{ K}$. However, this is still too cold to account for the X-ray flux.

Pure hydrogen (DA, series C) atmospheres produce by far the “hardest” possible spectrum, i.e. the highest X-ray flux for a given temperature. Again, these models lead to the situation that a relatively good fit to the PSPC PHD can be obtained at $T_{\text{eff}} \approx 100,000 \text{ K}$, but the $\text{He II } \lambda 1640$ line flux is only reproduced at $T_{\text{eff}} \lesssim 65,000 \text{ K}$.

Next, we assumed that helium is the main constituent of the hot component’s atmosphere. We examined DO/DOA model atmospheres with different helium-to-hydrogen ratios. The best solution to both, the UV and X-ray measurements is obtained with $\text{He/H} = 100$, $\text{C/H} = 0.1$, and $T_{\text{eff}} = 130,000 \text{ K}$ (Fig. 2, model D). If the hydrogen column density is chosen so that the lowest channels of the pulse height distribution are reproduced then the predicted flux is somewhat too small at higher energies. This deviation is larger for all other combinations of helium and carbon abundances (see Fig. 2). In the atmosphere of a hot DO white dwarf with $T_{\text{eff}} > 100,000 \text{ K}$ nitrogen, oxygen, and iron group elements may also be present. However, if we assume metal abundances as high

as in PG 1034+001 ($T_{\text{eff}} \approx 100,000 \text{ K}$, Werner et al. 1995a) the X-ray flux is completely absorbed.

Therefore an ionized spectrum is required

- with a strong $\text{He II } \lambda 228$ absorption edge in order to prevent moderately ionized lines like $\text{He II } \lambda 1640$ from becoming too strong.
- and a considerable portion of the energy released beyond the “gap” due to He II and possibly metals, to absorb high-energy photons.

5.3. Models with a stellar wind

If we assume that the hot object in SMC3 has a stellar wind we have to determine three model parameters, one more – the mass loss rate – in addition to effective temperature and stellar radius. As pointed out in Sect. 4, the stellar wind allows to suppress the He^+ ionizing photons even for very high stellar temperatures. With three model parameters — T_{eff} , R_* , and \dot{M} / v_{∞} — and three observational constraints — the continuum flux at 1300 \AA , the flux of the $\text{He II } \lambda 1640$ line, and the X-ray emission — it should be possible, in principle, to determine a solution.

However, in practice, we find that no unique solution exists. The problem is that if we fit both UV constraints, the 1300 \AA continuum and the $\text{He II } \lambda 1640$ line flux by adjusting two of the three parameters, say R_* , and \dot{M} / v_{∞} as a function of T_{eff} , we find that the predicted X-ray flux depends on the third parameter, T_{eff} , only in a limited range of temperatures: In particular, we find that for lower temperatures ($\approx 100 - 200 \text{ kK}$) the X-ray flux is quite sensitive to T_{eff} ; at higher temperatures, however, a saturation effect occurs and we obtain an upper limit to the predicted X-ray luminosity, almost regardless of the specified effective temperature.

It turns out that this upper limit reproduces almost, but not perfectly, the observed X-ray spectrum. The reason for this result is a typical property of a stellar wind. The wind that suppresses the photons at the the He^+ ionization edge is still relatively opaque in the observed X-ray region below 100 \AA . This is simply because the bound-free continuum cross section is proportional to λ^3 . Therefore, as long as we have a stellar temperature where the maximum of the radiation is in the observed X-ray or beyond, we find that all models have similar X-ray energy distribution determined by the helium absorption cross section. This is similar to adjusting the interstellar column density N_{H} . All these arguments are only valid for the energy spectrum around 100 \AA (where the bulk of the observed X-ray flux originates). The high energy tail, where the influence on the helium bound-free absorption becomes smaller, would in principle be very sensitive to the temperature. However, as discussed below, the presence of carbon absorbs all flux below 31.6 \AA .

Our difficulty to determine a unique set of the three parameters T_{eff} , R_* , and dM/dt does not prevent us to determine the stellar luminosity. We have stated above that

the form of the energy distribution is well determined and therefore, since we know the distance to our object, we know the luminosity with only a weak dependence on the other parameters. The statement that the effective temperature is not well known, is physically speaking a limit in determining the hydrostatic radius of the hot object, because this radius is hidden by the stellar wind. From models r and s (see Table 3, Fig. 3) that yield the best fit to the observations, we find $L_{\text{SMC3}} = 10^{4.05 \pm 0.05} L_{\odot}$.

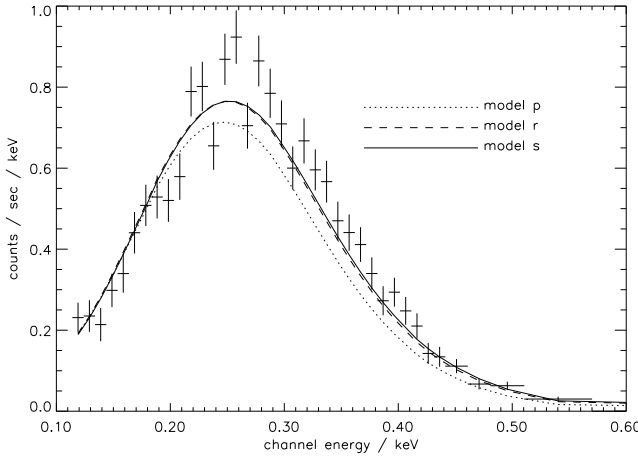


Fig. 3. Comparison of the observed PHD of SMC3 with three Wolf-Rayet type models with $T_{\text{eff}} = 220$ kK (model p, see Table 2 for the other parameters), 309 kK (r), and 354 kK (s). The predicted flux from model p is not hard enough to reproduce the observation, while the two hotter models (r) and (s) lead to relatively good fit to the data

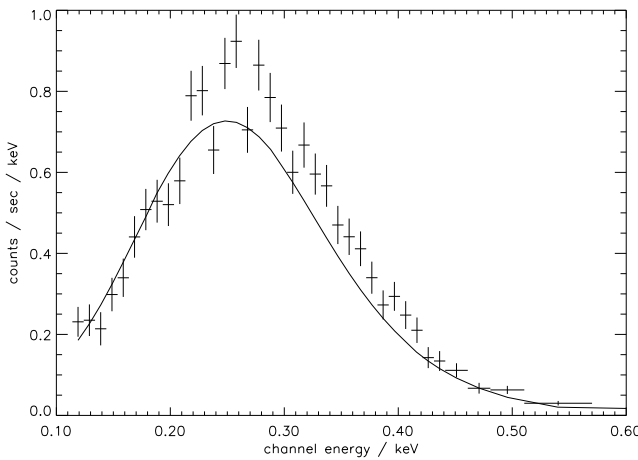


Fig. 4. The “coolest” Wolf-Rayet type model with $T_{\text{eff}} = 260$ K (q) that is able to reproduce the observed ROSAT PHD reasonably well

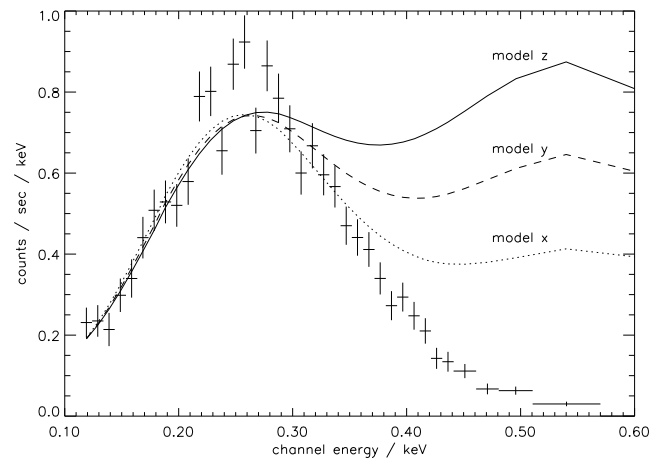


Fig. 5. Predicted ROSAT PHD for the models with different mass-loss rates shown in Fig. 1: $M_x = 10^{-5.1} M_{\odot}/\text{yr}$, $M_y = 10^{-5.2} M_{\odot}/\text{yr}$, and $M_z = 10^{-5.3} M_{\odot}/\text{yr}$; $v_{\infty} = 1000 \text{ km/sec}$ is assumed

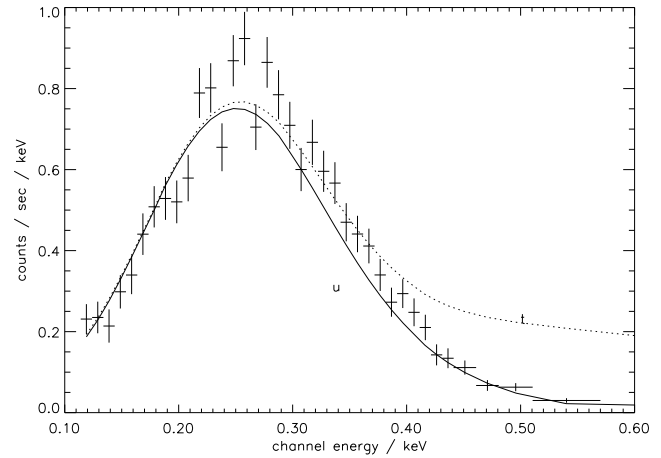


Fig. 6. These wind models with $T_{\text{eff}} \approx 270$ kK (model t and u) show, that too much hard X-ray photons are predicted if the carbon abundance is too low ($\text{C/He} = 2 \cdot 10^{-4}$ in the case of t compared to and $4 \cdot 10^{-4}$ for u)

Although we cannot decide which temperature is to be preferred, $T_{\text{eff}} = 309$ kK, 354 kK, or even hotter, we can set a lower limit to the effective temperature, i.e. an upper limit to the stellar radius. In Fig. 3 we show fits to the observed X-ray data based on models with effective temperatures of $T_{\text{eff}} = 220$ kK (model p), 309 kK (r), and 354 kK (s). It is evident that the radiation of the model p is not quite hard enough to reproduce the observed pulse height distribution. On the other hand, both hotter models come close to fitting the observed X-rays. Fig. 4 shows

that a model with $T_{\text{eff}} = 265$ kK (model q) is the coolest to fit the energy distribution of the hot object in SMC3 reasonably well.

In order to derive M a value for v_{∞} is required. Unfortunately, v_{∞} is not easily measurable. We do not dispose of the high S/N, high resolution UV spectra which allow to detect broad line components and determine their width. Even for galactic objects the velocity of the winds from hot components of symbiotic systems could be measured only for a few objects. Nussbaumer et al. (1995) and Nussbaumer & Vogel (1995) derive $v_{\infty} \approx 1000$ km/s which we will adopt in the following for SMC3. With this value, model q implies a rather high mass loss rate of $\dot{M} > 10^{-5.3} M_{\odot} \text{ yr}^{-1}$.

Helium and carbon are the only elements that have a significant influence on the resulting spectrum. Helium is needed in order to produce the absorption at the He^+ edge. The mass loss rate quoted above is basically the mass loss of helium. We have assumed a hydrogen abundance of 20 % by mass, but the hydrogen abundance could be changed arbitrarily without observable consequences. The carbon abundance is found to be very important. With the hot temperatures of our best fitting models we predict significant flux shortwards of the C^{+4} ionization edge at 31.6 Å (0.39 keV). Such energy distributions would produce much larger count rates than observed at energies larger than 0.4 keV. Therefore a relatively high carbon abundance is required in order to fit the observed energy distribution. Basically, we are invoking the same wind absorption effect at the C^{+4} edge as we invoked above to reduce the numbers of He^+ ionizing photons. Fig. 6 demonstrates the importance of the carbon edge by comparing the predicted ROSAT PHD for $\text{C}/\text{He}=2 \cdot 10^{-4}$ (too much "hard" X-ray flux) and $4 \cdot 10^{-4}$ (slightly too low flux at $E > 0.3$ keV) for about the same effective temperature (≈ 270 kK). A slightly larger relative carbon abundance is required to suppress the high energy photons for the hotter models. Therefore this carbon abundance is a minimum value and we cannot exclude higher values.

6. Conclusions

SMC3 is extraordinary, even among symbiotic stars. It is remarkably X-ray bright and shows unusually high ionization in the nebula. We succeeded to model these properties and the UV flux with a very hot WR-type model atmosphere. Our result clearly confirms that at least some of the supersoft X-ray sources contain very hot photospheres of degenerate stars. It shows in particular, that such hot stars can be encountered in symbiotic binary systems. Reasonable fits are achieved at temperatures above 260 000 K and mass-loss rates of $\dot{M} \gtrsim 1 \cdot 10^{-6} M_{\odot}/\text{yr}$, (assuming $v_{\infty} = 1000$ km/sec). Due to the properties of the wind models (the hot star itself is hidden by the stellar wind) no upper limit for the effective temperature could

be specified. However, this uncertainty does not effect the total luminosity: $L_{\text{SMC3}} = 10^{4.05 \pm 0.05} L_{\odot}$.

Even the lower limit for the effective temperature is extraordinarily high (see the temperature distribution for hot components of symbiotic systems in Fig. 7 of Paper III). To our knowledge SMC3 has the hottest stellar atmosphere ever derived in a sophisticated NLTE analysis. Until now, the hottest known (pre-) white dwarfs are the DA central star of the planetary nebula WDHS1 with $T_{\text{eff}}=160 \dots 200$ kK (Liebert et al. 1994; Napiwotzki 1995) and the PG1159 stars H1504+65 (Werner 1991) and RXJ2117+3412 (Werner et al. 1995b) with $T_{\text{eff}}=170$ kK. Note, however, that the temperature of SMC3 refers to the hydrostatic radius R_* and not to $\tau_R = 2/3$.

On the basis of LTE model atmospheres Heise et al. (1994) have shown that the ROSAT PSPC observations of the super-soft X-ray source 1E0056.8-7154, associated with the planetary nebula N67 (Wang 1991; Cowley et al. 1995) can be explained assuming a hot pre-white dwarf with an effective temperature as high as 450 kK. However, at such high temperatures NLTE effects are expected to be strong so that this result has to be checked using NLTE model atmospheres.

Strong mass loss is indispensable to explain the spectrum of SMC3. Direct or indirect signatures of strong mass loss are also encountered in other symbiotic novae (see Sion et al. 1993, JMW, Nussbaumer et al. 1995, Nussbaumer & Vogel 1995, and the discussion in Mürset et al. 1995a). If SMC3 has been shedding its wind constantly since the beginning of the outburst, it must have lost at least a mass of $\Delta M \sim 10^{-4} M_{\odot}$. This is much larger than the mass burnt during the same time, which means that the duration of the outburst of SMC3 will be limited rather by the mass loss than by the nuclear processes. ΔM is also a lower limit to the mass of the layer accreted by the white dwarf prior to outburst.

Kenyon et al. (1993), Mürset & Nussbaumer (1994), and JMW found for the known galactic symbiotic novae luminosities clearly below the Eddington limit. This result is now confirmed with a result that, due to the well known distance, is probably more reliable than the galactic ones. Here we encounter a basic difference between symbiotic and classical novae which seem to exceed the Eddington limit (Starrfield et al. 1993; Shore, personal communication). If a core-mass – luminosity relation holds for the symbiotic novae we can derive a mass $M \approx 0.8 M_{\odot}$ for the hot star (with the relation from Joss et al. 1987).

As a final comment we would like to stress that a photospheric X-ray source like SMC3 can only be reasonably investigated with i) multi-frequency data and ii) sophisticated non-LTE atmosphere models. Kahabka et al. (1994) impressively demonstrated the failure of black body fits to the ROSAT PHD by deriving a luminosity of $L \sim 10^{13} L_{\odot}$ for SMC 3. The reasons for the failure are obvious: Fitting the ROSAT data alone is a dangerous extrapolation, because they represent only an extreme tail of the stel-

lar spectrum. Even worse, this extreme part is exactly the spectral region where hot atmospheres differ very strongly from Planck curves.

Acknowledgements. We thank Steven N. Shore for helpful comments. Work on ROSAT data in Kiel is supported by DARA grant 50 OR 94091. KW acknowledges support by the DFG under grant We1312/6-1.

References

Aufdenberg J.P., 1993, *ApJS* 87, 337

Barnes T.G., Moffett T.J., Gieren W.P., 1993, *ApJ* 405, L51

Bessell M.S., 1991, *A&A* 242, L17

Cowley A.P., Schmidtke P.C., Hutchings J.B., Crampton D., 1995, *PASP* 107, 927

Cruddace R., Paresce F., Bowyer S., Lampton M., 1974, *ApJ* 187, 497

Davidson A., Malina R., Bowyer S., 1977, *ApJ* 211, 866

Deuel W., 1986, in: *Workshop on Model Nebulae*, ed. D. Pé quignot, *Publ. Obs. de Paris-Meudon*, p. 122

Groenewegen M.A.T., Lamers H.J.G.L., 1989, *A&AS* 79, 359

Hamann W.-R., Schmutz W., 1987, *A&A* 174, 173

Hasinger G., 1994, *Rev. in Modern Astron.* 7, ed. G. Klare, *Astronomische Gesellschaft*, p. 129

Heise J., van Teeseling A., Kahabka P., 1994, *A&A* 288, L45

Herbig G.H., Hoffleit D., 1975, *ApJ* 202, L41

Hummer D.G., Storey P.J., 1987, *MNRAS* 224, 801

Jordan S., Mürset U., Werner K., 1994a, *A&A* 283, 475 (JMW)

Jordan S., Wolff B., Koester D., Napiwotzki R., 1994b, *A&A* 290, 834

Joss P.C., Rappaport S., Lewis W., 1987, *ApJ* 319, 180

Kahabka P., Pietsch W., 1993, in: *New Aspects of Magellanic Cloud Research*, eds. B. Baschek, G. Klare, J. Lequeux, Springer, p. 71

Kahabka P., Pietsch W., Hasinger G., 1994, *A&A* 288, 538

Kenyon S.J., Mikołajewska J., Mikołajewski M., Polidan R.S., Slovak M.H., 1993, *AJ* 106, 1573

Liebert J., Bergeron P., Tweedy R.W., 1994, *ApJ* 424, 817

Morgan D.H., 1992, *MNRAS* 258, 639

Morrison R., McCammon D., 1983, *ApJ* 270, 119

Mürset U., Nussbaumer H., 1994, *A&A* 282, 586

Mürset U., Nussbaumer H., Schmid H.M., Vogel M., 1991, *A&A* 248, 458

Mürset U., Jordan S., Walder R., 1995a, *A&A* 297, L87

Mürset U., Schild H., Vogel M., 1995b, *A&A*, in press (Paper III)

Napiwotzki R., 1995, in: *White Dwarfs*, eds. D. Koester and K. Werner, *Lecture Notes in Physics* No. 443, Springer, Berlin, p. 176

Nussbaumer H., Schild H., 1981, *A&A* 101, 118

Nussbaumer H., Vogel M., 1995, *A&A*, in press

Nussbaumer H., Schmutz W., Vogel M., 1995, *A&A* 293, L13

Pauldrach A., Puls J., Kudritzki R.P., 1986, *A&A* 164, 86

Pietsch W., Kahabka P., 1993, in: *New Aspects of Magellanic Cloud Research*, eds. B. Baschek, G. Klare, J. Lequeux, Springer, p. 59

Prévot M.L., Lequeux J., Maurice E., Prévot L., Rocca-Volmerange B., 1984, *A&A* 132, 389

Schaerer D., Schmutz W., 1995, *A&A* 288, 231

Schmid H.M., 1989, *A&A* 211, L31

Schmutz W., Hamann W.-R., Wessolowski U., 1989, *A&A* 210, 236

Schmutz W., Leitherer C., Gruenwald R., 1992, *PASP* 104, 1164

Sion E.M., Shore S.N., Ready C.J., Scheible M.P., 1993, *AJ* 106, 2118

Sion E.M., Starrfield S.G., 1994, *ApJ* 421, 261

Starrfield S., Hauschildt P.H., Shore S.N., Sonneborn G., Gonzales-Riestra G., Sparks W.M., 1993, in: *New Aspects of Magellanic Cloud Research*, eds. B. Baschek, G. Klare, J. Lequeux, *Lecture Notes in Physics* 416, Springer, p. 181

Vogel M., 1990, Ph.D. thesis, ETH-Zürich, No. 9089

Vogel M., Morgan D.H., 1994, *A&A* 288, 842 (Paper I)

Wang Q., 1991, *MNRAS* 252, 47p

Webster B.L., Allen D.A., 1975, *MNRAS* 171, 171

Werner K., 1991, *A&A* 251, 147

Werner K., Heber U., 1991, in: *Stellar Atmospheres: Beyond Classical Models*, *NATO ASI Series C*, Vol. 341, eds. L. Crivellari, I. Hubeny and D.G. Hummer, Kluwer, Dordrecht, p. 341

Werner K., Dreizler D., Wolff B., 1995a, *A&A* 298, 567

Werner K., Dreizler D., Heber U., Rauch T., Fleming T.A., Sion E.M., Vauclair G., 1995b, *A&A*, in press

Wessolowski U., Schmutz W., Hamann W.-R., 1988, *A&A* 194, 160

Wolff B., Jordan S., Koester D., 1996, *A&A*, in press

Zimmermann H.U., Becker W., Belloni T., Döbereiner S., Izzo C., Kahabka P., Schwentker O., 1994, *EXSAS User's Guide*, MPE Report 257